

## The K-doped $g\text{-C}_3\text{N}_4$ decorated with $\text{Ti}_3\text{C}_2$ for efficient photocatalytic $\text{H}_2\text{O}_2$ production

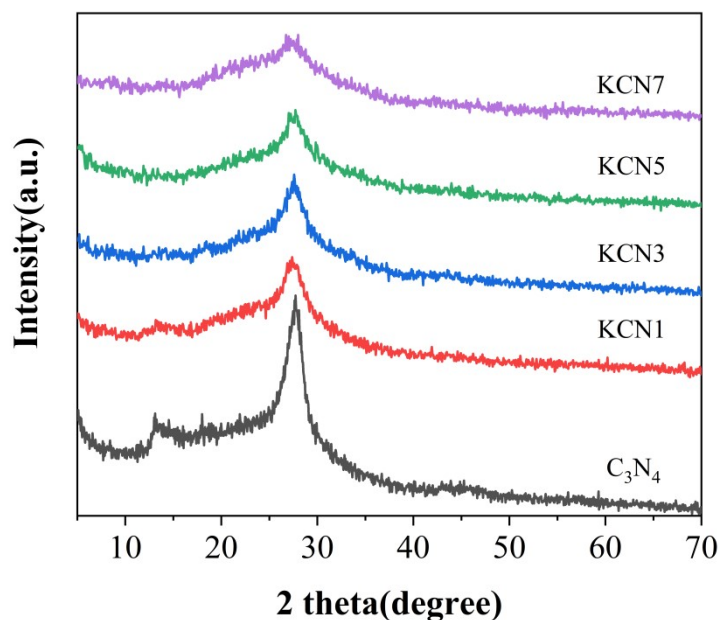


Figure S1. XRD patterns of KCN at different amounts.

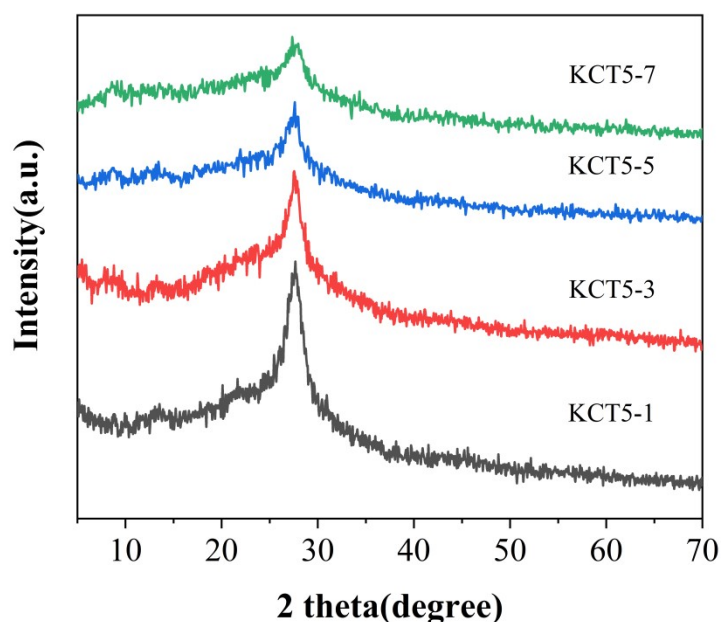
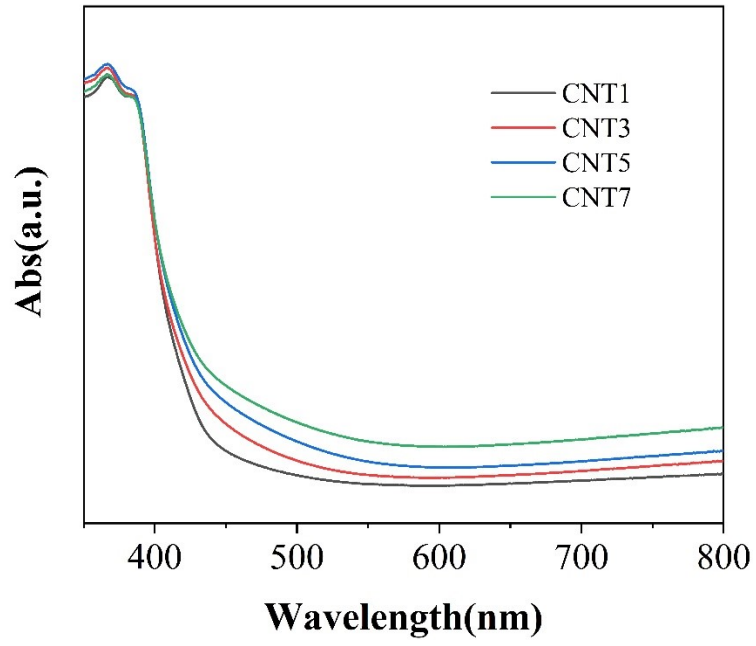
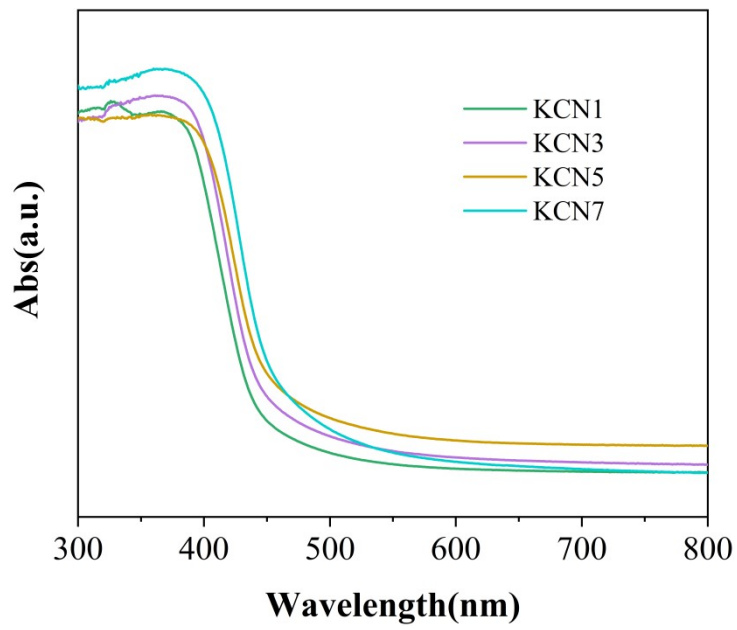


Figure S2. XRD patterns of KCT5-X at different amounts.



**Figure S3.** UV-visible diffuse reflection spectrum of CNTX.



**Figure S4.** UV-visible diffuse reflection spectrum of KCNX.

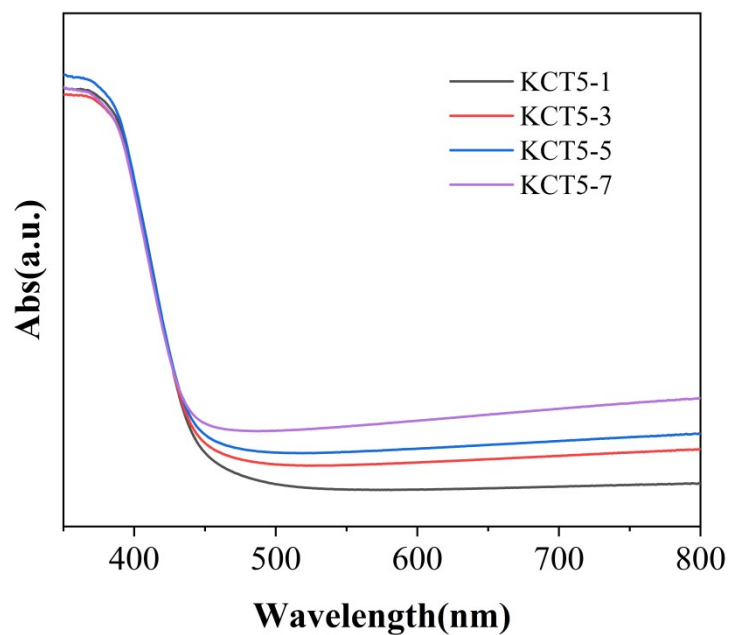


**Figure S5.** UV-visible diffuse reflection spectrum of KCT5-X.

**Table S1.** Specific surface area, pore volume and average pore size of g-C<sub>3</sub>N<sub>4</sub>, CNT5, KCN5, KCT5-5

| Sample                          | $S_{\text{BET}}$ (m <sup>2</sup> /g) | Pore volume (cm <sup>3</sup> /g) | Average pore size (nm) |
|---------------------------------|--------------------------------------|----------------------------------|------------------------|
| g-C <sub>3</sub> N <sub>4</sub> | 81.77                                | 0.51                             | 21.26                  |
| CNT5                            | 59.13                                | 0.29                             | 25.35                  |
| KCN5                            | 22.10                                | 0.11                             | 21.29                  |
| KCT5-5                          | 25.76                                | 0.12                             | 19.73                  |

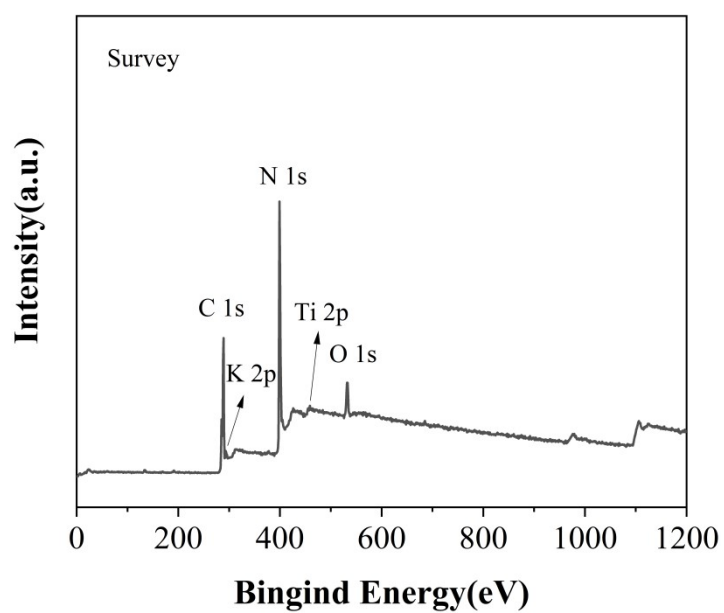


**Figure S6.** XPS spectra of KCT5-5 sample

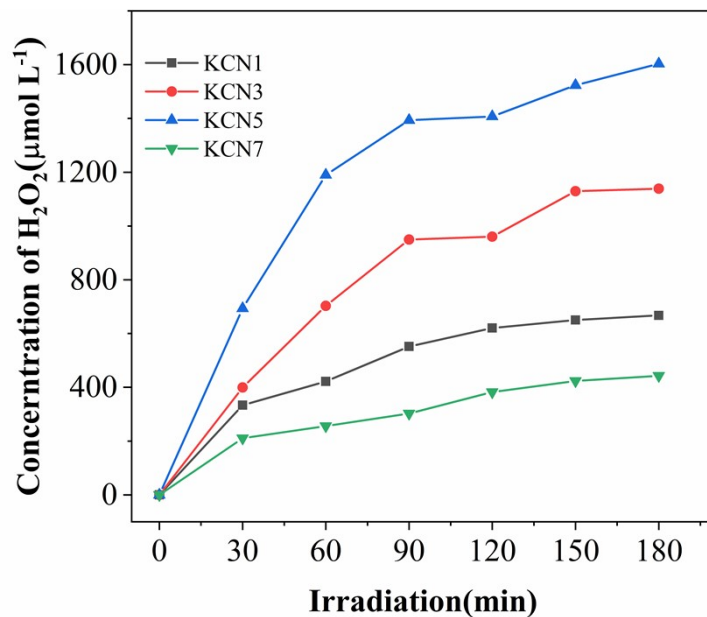


**Figure S7.** Photocatalytic H<sub>2</sub>O<sub>2</sub> production under visible light irradiation at KCN<sub>x</sub>.

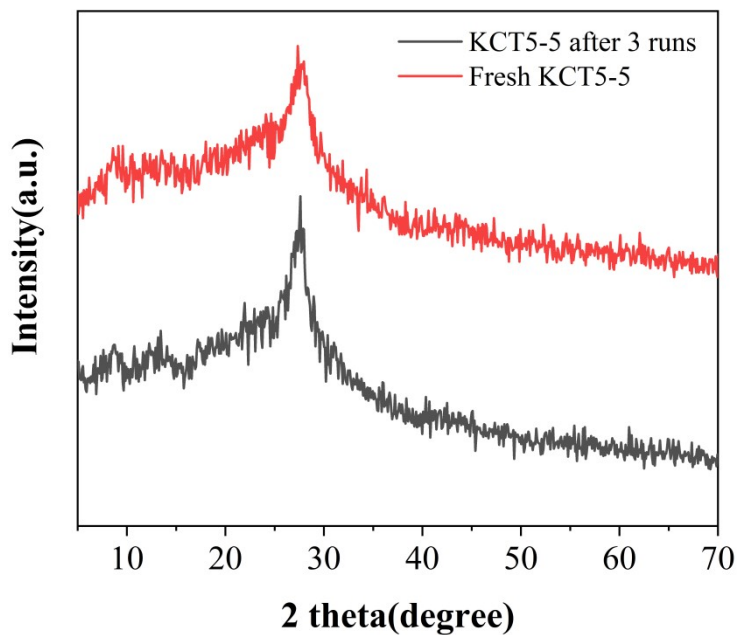


**Figure S8.** XRD patterns of KCT5-5 before and after cycle testing.

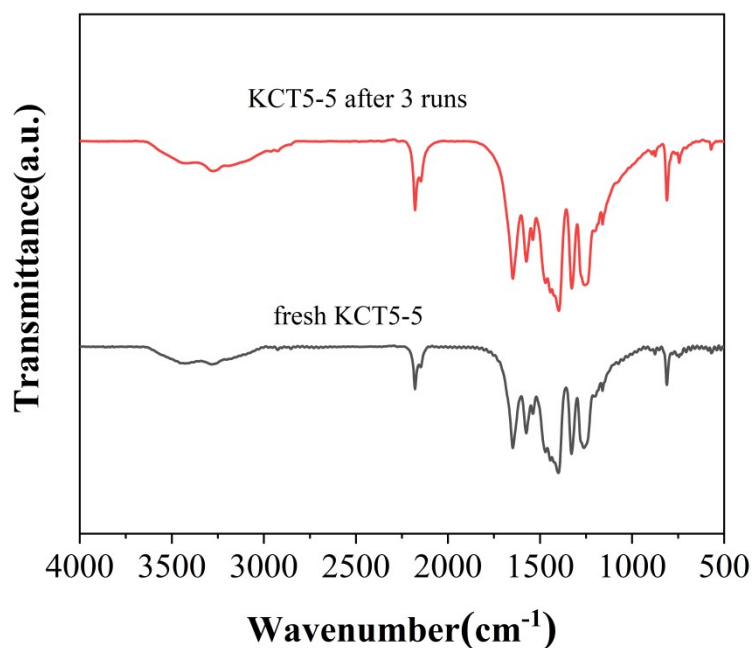


**Figure S9.** FTIR spectra of KCT5-5 before and after cycle testing.

**Table S2.** Fitted decay time constants of CN, CNT5, KCN5 and KCT5-5 from TRPL spectra.

|        | $\tau_1/\text{ns}$ | $A_1$    | $\tau_2/\text{ns}$ | $A_2$ | $\tau_n/\text{ns}$ |
|--------|--------------------|----------|--------------------|-------|--------------------|
| CN     | 1.03               | 84708.58 | 6.44               | 0.71  | 1.03               |
| CNT5   | 1.39               | 3919.54  | 8.39               | 0.83  | 1.40               |
| KCN5   | 1.59               | 1438.28  | 7.46               | 1.18  | 1.61               |
| KCT5-5 | 0.65               | 71.81    | 3.45               | 18.15 | 2.25               |

$$\tau_n = (A_1\tau_1^2 + A_2\tau_2^2) / (A_1\tau_1 + A_2\tau_2)$$

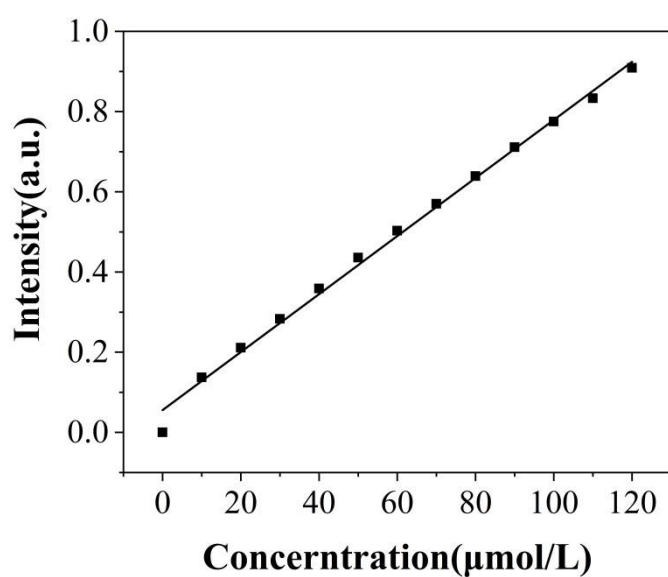


**Figure S10.** Measuring the concentrations of generated  $\text{H}_2\text{O}_2$  by iodometry.

**Table S3.** Calculated  $K_f$  and  $K_d$  values of CN, CNT5, KCN5 and KCT5-5.

|        | $K_f$ ( $10^1 \mu\text{mol L}^{-1} \text{min}^{-1}$ ) | $K_d$ ( $10^{-3} \text{min}^{-1}$ ) |
|--------|---|-------------------------------------|
| CN     | 0.13  | 8.33                                |
| CNT5   | 0.41  | 5.57                                |
| KCN5   | 3.35  | 4.34                                |
| KCT5-5 | 4.54  | 3.36                                |

**Table S4.** Comparison of  $\text{H}_2\text{O}_2$  production rates achieved by recently reported photocatalytic systems

| Photocatalysts  | Reaction solution | $\text{H}_2\text{O}_2$ yield ( $\mu\text{mol g}^{-1} \text{h}^{-1}$ ) | Ref.      |
|---|-------------------|---|-----------|
| MIL-125-NH <sub>2</sub>   | BNOH              | 800   | [1]       |
| Cu-doped g-C <sub>3</sub> N <sub>4</sub>                                | Water             | 1130  | [2]       |
| Ti <sub>3</sub> C <sub>2</sub> QDs/g-C <sub>3</sub> N <sub>4</sub>      | EA                | 560.7   | [3]       |
| Mn <sub>3</sub> O <sub>4</sub> /Co <sub>9</sub> S <sub>8</sub>          | Water             | 270   | [4]       |
| S-doped-C/CdS   | Water             | 712.5   | [5]       |
| Thiourea functionalized CTF   | Water             | 653.62  | [6]       |
| KH <sub>2</sub> PO <sub>4</sub> /g-C <sub>3</sub> N <sub>4</sub>        | 10%EA             | 500   | [7]       |
| KPF6-C <sub>3</sub> N <sub>4</sub>                                      | EA                | 300   | [8]       |
| ZnO nanorods  | EA                | 285   | [9]       |
| K-doped g-C <sub>3</sub> N <sub>4</sub> /Ti <sub>3</sub> C <sub>2</sub> | 10%IPA            | 1136.67   | This work |

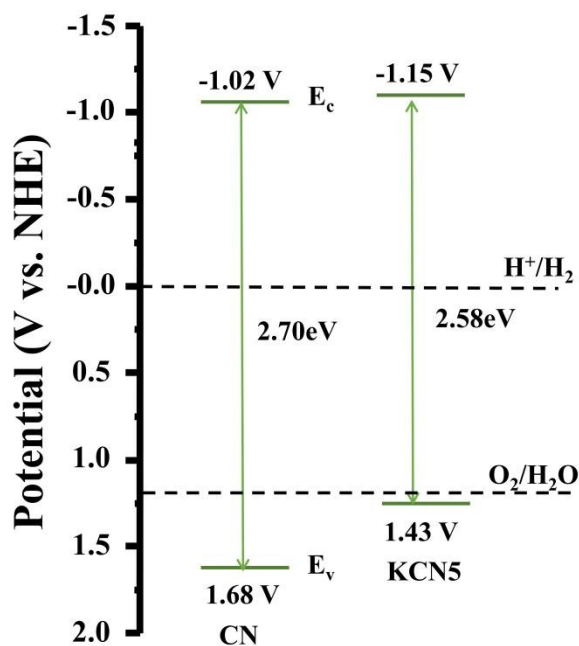


**Figure S11.** Schematic illustration of the band structure of CN and KCN5.

## Reference

- [1] Isaka Y, Kawase Y, Kuwahara Y, et al. Two-phase system utilizing hydrophobic metal–organic frameworks (MOFs) for photocatalytic synthesis of hydrogen peroxide[J]. *Angewandte Chemie International Edition*, 2019, 58(16): 5402-5406.
- [2] Hu S, Qu X, Li P, et al. Photocatalytic oxygen reduction to hydrogen peroxide over copper doped graphitic carbon nitride hollow microsphere: The effect of Cu(I)-N active sites[J]. *Chemical Engineering Journal*, 2018, 334: 410-418.
- [3] Lin S, Zhang N, Wang F, et al. Carbon vacancy mediated incorporation of Ti<sub>3</sub>C<sub>2</sub> quantum dots in a 3D inverse opal g-C<sub>3</sub>N<sub>4</sub> Schottky junction catalyst for photocatalytic H<sub>2</sub>O<sub>2</sub> production[J]. *ACS Sustainable Chemistry & Engineering*, 2021, 9(1): 481-488.
- [4] Zhang H, Bai X. Photocatalytic production of hydrogen peroxide over Z-scheme Mn<sub>3</sub>O<sub>4</sub>/Co<sub>9</sub>S<sub>8</sub> with p-n heterostructure[J]. *Applied Catalysis B: Environmental*, 2021, 298: 120516.
- [5] Lee J H, Cho H, Park S O, et al. High performance H<sub>2</sub>O<sub>2</sub> production achieved by sulfur-doped carbon on CdS photocatalyst via inhibiting reverse H<sub>2</sub>O<sub>2</sub> decomposition[J]. *Applied Catalysis B: Environmental*, 2021, 284: 119690.
- [6] Wu C, Teng Z, Yang C, et al. Polarization engineering of covalent triazine frameworks for

highly efficient photosynthesis of hydrogen peroxide from molecular oxygen and water[J].  
Advanced Materials, 2022, 34(28): 2110266.

- [7] Tian J, Wu T, Wang D, et al. One-pot synthesis of potassium and phosphorus-doped carbon nitride catalyst derived from urea for highly efficient visible light-driven hydrogen peroxide production[J]. Catalysis Today, 2019, 330: 171-178.
- [8] Kim S, Moon G-h, Kim H, et al. Selective charge transfer to dioxygen on KPF6-modified carbon nitride for photocatalytic synthesis of H<sub>2</sub>O<sub>2</sub> under visible light[J]. Journal of Catalysis, 2018, 357: 51-58.
- [9] Jiang Z, Zhang Y, Zhang L, et al. Effect of calcination temperatures on photocatalytic H<sub>2</sub>O<sub>2</sub>-production activity of ZnO nanorods[J]. Chinese Journal of Catalysis, 2022, 43(2): 226-233.